JOURNAL OF MATERIALS SCIENCE 16 (1981) 1356–1366

Crystallographic analysis in the transmission electron microscope

L. P. STOTER*
H. H. Wills Physics Laboratory, Royal Fort, Tyndal Avenue, Bristol, UK

Analysis of the symmetry elements present in electron diffraction patterns produced by the convergent beam technique allows rapid determination of the crystallographic point group. Useful space group information is obtainable from the same patterns. The technique is particularly useful in the study of precipitates and is illustrated with examples from AISI Type 316 stainless steel.

1. Introduction

The transmission electron microscope (TEM) technique of convergent beam diffraction has been known for many years [1] but until recently instrumental deficiencies have severely limited its usefulness and application. Now that a number of commercial instruments capable of convergent beam diffraction have become available the technique deserves wider usage. This paper attempts to outline the application of convergent beam diffraction methods to crystallographic analysis, particularly point group determination, so that a microscopist not conversant with the technique or the underlying theory can appreciate its usefulness, grasp an understanding of its application and begin to apply the technique.

Convergent beam (CB) diffraction methods have a number of attractive advantages when compared with more conventional approaches. The configuration of the electron beam is such that diffraction information can be obtained from very small areas (~ 10 nm) and with confidence that it comes from a known location. The electron beam configuration is similar to that required for energy dispersive X-ray analysis (EDX) so that both techniques can be used together without difficulty. The CB patterns obtained are highly characteristic of the particular phase from which they come, to such an extent that a single zone axis pattern (ZAP) from an already characterized phase will provide positive identification. The patterns are extremely sensitive to changes in lattice parameter and given ideal circumstances it is possible to detect a lattice parameter change as small as a few parts in 10^4. This makes it possible to detect strain in a specimen or small compositional changes, too small to be detectable by EDX. The CB patterns are also sensitive to thickness and it is possible, in some cases, for two patterns differing only in that they come from different thicknesses of the same phase to be attributed by the inexperienced to different phases. In the simpler crystal structures the variation in the patterns can be used to obtain measurements of thickness.

A good general introduction to convergent beam diffraction is given by Steeds [2]. Buxton *et al.* [3] give detailed theory and comprehensive information on relating convergent beam pattern (CBP) symmetry elements to point groups. Steeds *et al.* [4] provide a brief guide on how to obtain space group information from CBPs. However, none are a practical guide on how to start using the technique for crystallographic studies in materials science or metallurgy. It is hoped that this paper will provide such a guide.

2. What is a convergent beam pattern (CBP)?

A typical CBP of a low index zone axis is shown in Fig. 1. The discs correspond to the points of the conventional diffraction pattern and may be indexed in exactly the same way. The central, or bright-field disc is formed by electrons leaving the crystal in the same direction as incident electrons.

*Present address: Department of Metallurgy and Science of Materials, University of Oxford, Parks Road, Oxford.

0022–2461/81/051356–11$03.10/0

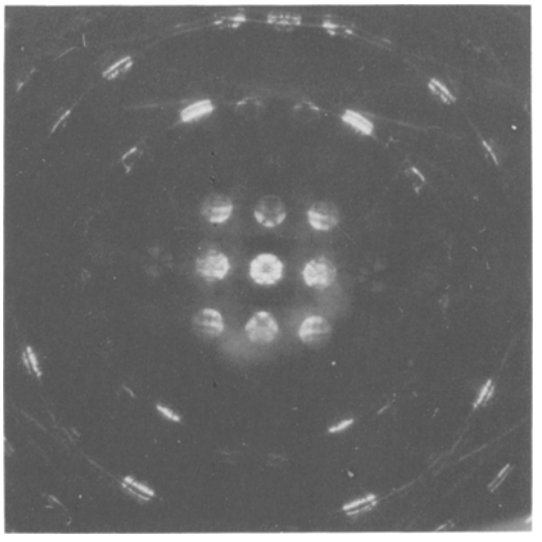

Figure 1 The [0 3 $\bar{3}$ 2] convergent beam zone axis pattern from Laves phase showing Kikuchi lines, hoLz lines, bright- and dark-field discs and a number of higher order Laue zones.

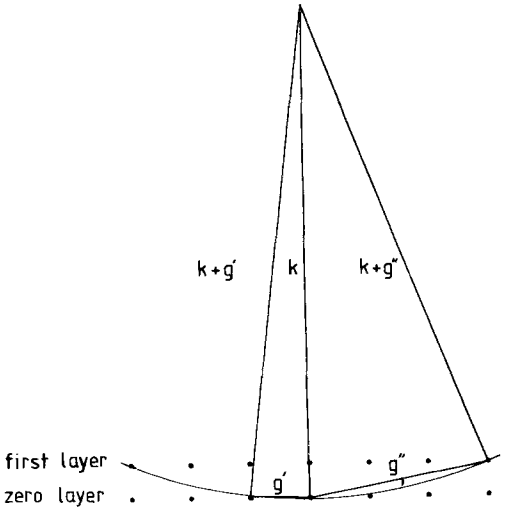

Figure 2 The Ewald sphere construction.

The remaining dark-field discs are formed by elastically scattered (i.e. diffracted) electrons. Each disc is a map of electron intensity transmitted by the crystal, for particular diffraction vectors **G**, as a function of angle. The angular range within the discs is the same as the angle of convergence of the incident electron beam and is about 1° (1.7×10^{-2} radians) or less.

The various features of a CBP are most easily understood by reference to the Ewald sphere construction, shown in Fig. 2. The broad light and dark areas within the disc result from interaction involving the zero layer only. At large angles from the incident direction CBPs often have one or more broken rings of intensity which arise from interactions with higher layers; the higher order Laue zones. These interactions can in turn affect the zero layer interactions, so producing the network of fine, dark lines visible in the zero layer bright-field and dark-field discs. These dark lines, the higher order Laue zone lines (hoLz lines) will often be parallel to one of the short, bright lines making up the higher order Laue zones. Thus by indexing the higher order Laue zones, it is often possible to index some of the hoLz lines in the bright-field disc. Overlaying the whole pattern is the familiar diffuse scatter produced by inelastic scattering of electrons which, when they in turn are elastically scattered, produce Kikuchi lines, as happens in conventional diffraction patterns.

3. How is a CBP produced?

The principle of CB diffraction is straightforward. As the name implies, the specimen is illuminated with a convergent beam of electrons, typically with an angle of convergence of about 1° (1.7×10^{-2} radians) or less and with a crossover diameter of 40 nm or less. Referring to a ray diagram (Fig. 3), it can be seen how this compares with conventional diffraction techniques, where the specimen is illuminated with a nearly parallel beam of electrons. In both cases the diffraction pattern is formed in the back focal plane of the objective lens. For conventional diffraction, the pattern is an array of points, each being the focus of a particular diffracted beam. For CB diffraction, the convergent incident beam results in the points being spread out into discs. In both cases the patterns are then transferred by intermediate and projector lens to the screen or photographic plate. In principle it should be possible, given a perfectly flat, parallel-sided crystal, to construct the CB pattern from a large number of conventional diffraction patterns taken at very slightly different specimen orientations. Of course in reality this is not possible or necessary.

The stringent instrumental requirements are met by most modern transmission electron microscopes which are suitable for STEM but the quality of the CBPs produced would vary between the different instruments. Not only is it necessary to be able to produce the required electron beam configuration but it is very important to have a good, high vacuum with a very low partial pressure

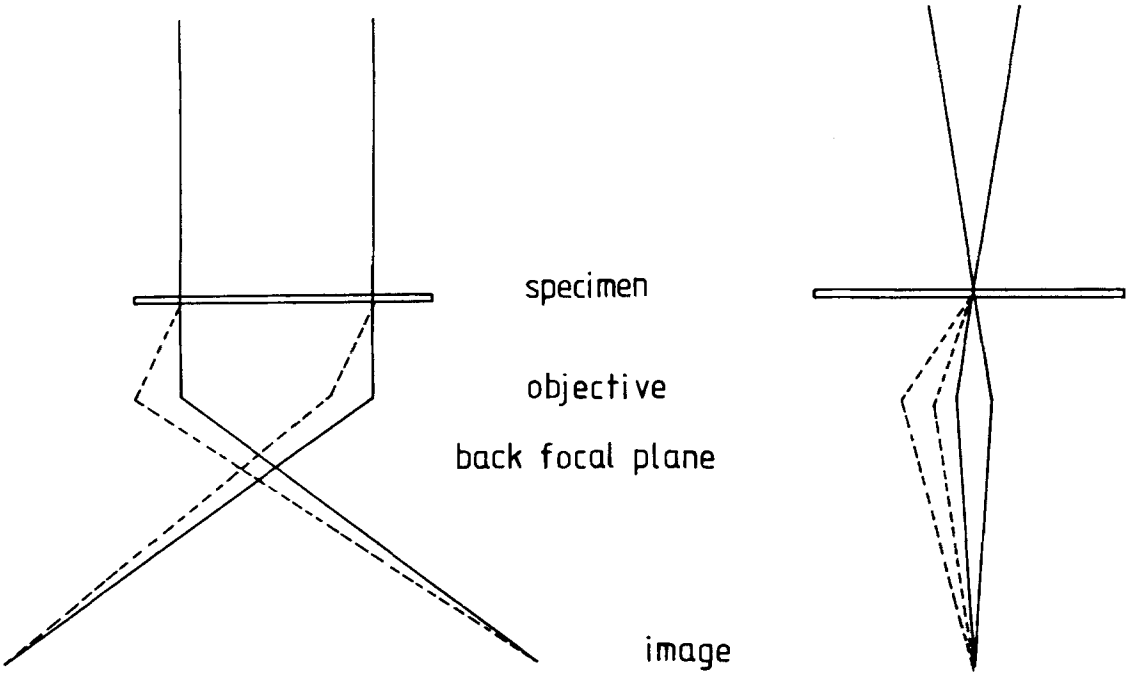

Figure 3 Ray diagrams illustrating conventional and convergent beam diffraction.

of hydrocarbons. An iongetter pump would probably be necessary to achieve the required vacuum. Where this requirement is not met contamination spots will rapidly form where the electron beam is focused on the specimen and the CB pattern is obliterated [5]. While the requirements of vacuum and electron beam configuration are sufficient to obtain good quality CB patterns, they are probably insufficient to make crystallographic analysis easy. In particular, a high tilt, eucentric goniometer specimen stage is useful. The ability to set a wide range of conditions on the first and second condenser lenses and objective lenses will improve the flexibility of the microscope.

It is necessary to be able to observe the bright-field and at least one or two dark-field discs so as to analyse the pattern symmetry. This sets a minimum on the angular field of view needed of the diffraction plane of the microscope. This minimum will of course vary depending on crystal lattice parameters and zone axis. However, for austenite the minimum useful angle is probably of the order of 3°. It is an advantage to be able to view much larger angles ($\sim 15°$) so that the higher order Laue zones can be clearly seen, since these often reveal the pattern symmetry more clearly than the zero layer. To obtain these large angles of view of the diffraction plane low camera lengths (< 300 mm) are necessary. Even then the field of view may be restricted by fixed apertures.

4. What to look for in CBPs

There are several different ways in which CBPs can be studied and used. On a very simple level they can be used as a way of "finger printing" different phases. This can be compared with the qualitative use of EDX analysis. Although the use of CBPs would be somewhat slower than EDX, it would be considerably more accurate. A common problem that arises in the study of stainless steels is confusion between sigma-phase and chi-phase when using EDX because of their similar compositions. No such problem occurs when using CB.

As a next step CBPs can be studied analytically in a geometrical fashion, to provide information about the symmetry in crystal structures. In this way crystallographic point groups can be determined.

The basic symmetry elements present in a CBP are mirror lines (m) and rotational symmetries (1, 2, 3, 4, 6). They may occur within the bright-field disc, within a dark-field disc, between certain dark-field discs or in the whole pattern. A systematic study of these symmetry relations allows the point group to be determined. The complexity of the situation means that the problem of actually determining the point group may be approached in several ways, there being no "correct" procedure to follow. In some cases it is very easy, with only two pieces of information being required, whereas in other cases extra information

TABLE I Pattern symmetries (published by permission of the Royal Society)

Diffraction group	Bright-field	Whole pattern	Dark-field		± G		Projection diffraction group
			General	Special	General	Special	
1	1	1	1	None	1	None	1_R
1_R	2	1	2	None	1	None	
2	2	2	1	None	2	None	
2_R	1	1	1	None	2_R	None	21_R
21_R	2	2	2	None	21_R	None	
m_R	m	1	1	m	1	m_R	
m	m	m	1	m	1	m	$m1_R$
$m1_R$	2mm	m	2	2mm	1	$m1_R$	
$2m_Rm_R$	2mm	2	1	m	2	—	
2mm	2mm	2mm	1	m	2	—	$2mm1_R$
2_Rmm_R	m	m	1	m	2_R	—	
$2mm1_R$	2mm	2mm	2	2mm	21_R	—	
4	4	4	1	None	2	None	
4_R	4	2	1	None	2	None	41_R
41_R	4	4	2	None	21_R	None	
$4m_Rm_R$	4mm	4	1	m	2	—	
4mm	4mm	4mm	1	m	2	—	$4mm1_R$
4_Rmm_R	4mm	2mm	1	m	2	—	
$4mm1_R$	4mm	4mm	2	2mm	21_R	—	
3	3	3	1	None	1	None	31_R
31_R	6	3	2	None	1	None	
$3m_R$	3m	3	1	m	1	m_R	
3m	3m	3m	1	m	1	m	$3m1_R$
$3m1_R$	6mm	3m	2	2mm	1	$m1_R$	
6	6	6	1	None	2	None	
6_R	3	3	1	None	2_R	None	61_R
61_R	6	6	2	None	21_R	None	
$6m_Rm_R$	6mm	6	1	m	2	—	
6mm	6mm	6mm	1	m	2	—	$6mm1_R$
6_Rmm_R	3m	3m	1	m	2_R	—	
$6mm1_R$	6mm	6mm	2	2mm	21_R	—	

Where a dash appears in column 7, the special symmetries can be deduced from columns 5 and 6 of this table.

may be necessary. Low symmetry point groups in particular involve more effort than high symmetry point groups.

It will become clear how easy the method is if examples are given. Four tables are shown and they can be used in various ways. The symbols are fully explained by Buxton *et al.* [3], who are the source of Tables I, II and III.

The use of the broad, zero layer detail for making thickness measurements is detailed by Shannon and Steeds [6] and the application of hoLz lines is included in the work of Jones *et al.* [7], who also deal in detail with the theory of hoLz lines. For the present paper it needs to be pointed out that the zero layer detail of CBPs only reflects the crystal symmetry as projected along the particular zone axis. This may be different from the true symmetry of the CBP and only allows point groups to be determined by looking at a relatively large number of zone axes. It is the hoLz lines which reflect the true three-dimensional symmetry of the crystal and thus those zone axes displaying hoLz lines are considerably more useful than those containing only projected symmetry information.

5. Obtaining a CBP

The following description is based on the Philips EM400 transmission electron microscope, in the STEM configuration. The basis is the same for other microscopes but will differ in detail.

In order to obtain a CBP from a crystal it is necessary to produce a small probe. This can be achieved in different ways. The easiest technique is to use only the condenser lenses to form the probe. This is done by first increasing the first condenser lens current to its maximum and then adjusting the second condenser lens current to

TABLE II Relation between the diffraction groups and the crystal point groups (published by permission of the Royal Society)

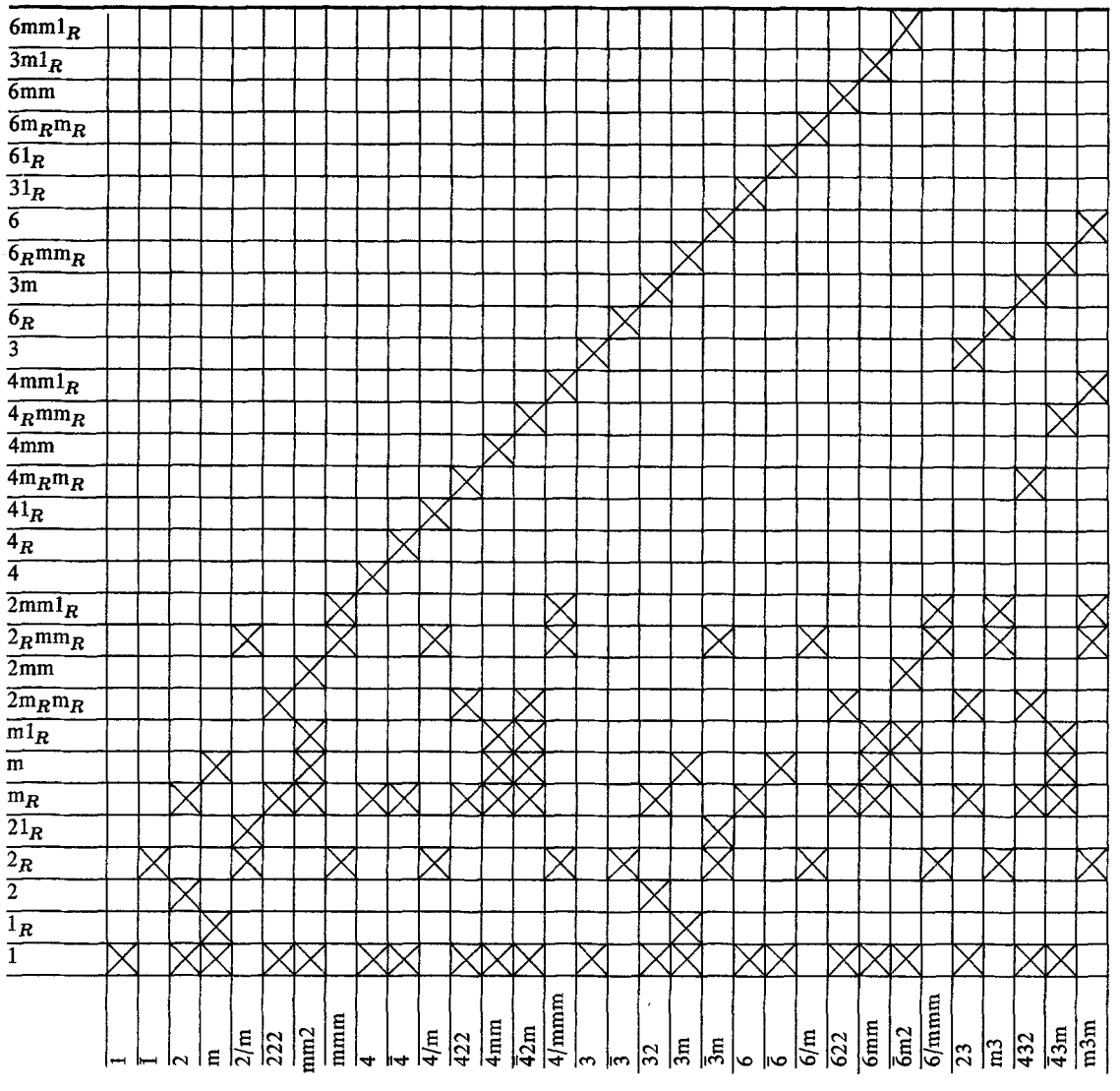

produce the small probe. The condenser astigmatism is best adjusted at this stage to produce a small, circular spot. The probe is located accurately on the specimen while still in the image mode. On going to diffraction an array of discs will be visible. Either side of the probe focus a shadow image of the specimen will be visible in these discs. As focus is approached the magnification of the shadow image increases and close to the focus the image is highly distorted. At focus all real space detail vanishes leaving a CBP. When orienting the specimen, it is best to work in the diffraction mode with the second condenser defocused so that the shadow image can be followed and the probe relocated exactly. Alignment exactly on a zone axis is difficult using the specimen tilt controls alone and final adjustment is best done by a small translation of the second condenser lens aperture, in effect a small tilt of the electron beam.

The use of only the condenser lenses to form the probe represents one extreme of operation. In the other extreme, the second condenser lens is switched off and the probe is formed using the first condenser lens and the objective lens. These two modes of operation are sometimes termed the "TEM mode" and the "STEM mode", respectively. In both modes the angle of convergence is determined by the diameter of the second condenser lens aperture, although for the same diameter aperture the "STEM mode" results in a larger

TABLE III Zone axis symmetries (published by permission of the Royal Society)

Point group	⟨111⟩	⟨100⟩	⟨110⟩	⟨*uvo*⟩	⟨*uuw*⟩	[*uvw*]
m3m	$6_R mm_R$	$4mm1_R$	$2mm1_R$	$2_R mm_R$	$2_R mm_R$	2_R
43m	3m	$4_R mm_R$	$m1_R$	m_R	m	1
432	$3m_R$	$4m_R m_R$	$2m_R m_R$	m_R	m_R	1

Point group	⟨111⟩	⟨100⟩	⟨*uv0*⟩	[*uvw*]
m3	6_R	$2mm1_R$	$2_R mm_R$	2_R
23	3	$2m_R m_R$	m_R	1

Point group	[0001]	⟨11$\bar{2}$0⟩	⟨1$\bar{1}$00⟩	[*uv.o*]	[*uu.w*]	[*u*$\bar{u}$.*w*]	[*uv.w*]
$\bar{6}$/mmm	$6mm1_R$	$2mm1_R$	$2mm1_R$	$2_R mm_R$	$2_R mm_R$	$2_R mm_R$	2_R
$\bar{6}$m2	$3m1_R$	$m1_R$	2mm	m	m_R	m	1
6mm	6mm	$m1_R$	$m1_R$	m_R	m	m	1
622	$6m_R m_R$	$2m_R m_R$	$2m_R m_R$	m_R	m_R	m_R	1

Point grou	[0001]	[*uv.o*]	[*uv.w*]
6/m	61_R	$2_R mm_R$	2_R
$\bar{6}$	31_R	m	1
6	6	m_R	1

Point group	[0001]	⟨11$\bar{2}$0⟩	[*u*$\bar{u}$.*w*]	[*uv.w*]
$\bar{3}$m	$6_R mm_R$	21_R	$2_R mm_R$	2_R
3m	3m	1_R	m	1
32	$3m_R$	2	m_R	1

Point group	[0001]	[*uv.w*]
$\bar{3}$	6_R	2_R
3	3	1

Point group	[001]	⟨100⟩	⟨110⟩	[*uvw*]	[*uvw*]	[*uuw*]	[*uvw*]
4/mmm	$4mm1_R$	$2mm1_R$	$2mm1_R$	$2_R mm_R$	$2_R mm_R$	$2_R mm_R$	2_R
$\bar{4}$2m	$4_R mm_R$	$2m_R m_R$	$m1_R$	m_R	m_R	m	1_R
4mm	4mm	$m1_R$	$m1_R$	m	m_R	m	1
422	$4m_R m_R$	$2m_R m_R$	$2m_R m_R$	m_R	m_R	m_R	1

Point group	[001]	[*uvw*]	[*uvw*]
4/m	41_R	$2_R mm_R$	2_R
$\bar{4}$	4_R	m_R	1
4	4	m_R	1

Point group	[001]	⟨100⟩	[*uvw*]	[*uvo*]	[*uvw*]
mmm	$2mm1_R$	$2mm1_R$	$2_R mm_R$	$2_R mm_R$	2_R
mm2	2mm	$m1_R$	m	m_R	1
222	$2m_R m_R$	$2m_R m_R$	m_R	m_R	1

Point group	[010]	[*uvw*]	[*uvw*]
2/m	21_R	$2_R mm_R$	2_R
m	1_R	m	1
2	2	m_R	1

Point group	[*uvw*]
$\bar{1}$	2_R
1	1

angle than the "TEM mode". It is also possible to work in an intermediate mode, where the angle of convergence also depends on the relative excitations of the second condenser and objective lenses.

The advantage of the STEM mode is that it allows considerably smaller probe diameters to be achieved. Its disadvantage is that since the objective is used in forming the probe, switching between diffraction and imaging condition necessitates repeated refocusing of the objective. In the TEM mode this problem is avoided since the objective is at the same excitation in both conditions. However the penalty is an increase in the minimum probe diameter. The various modes of operation are discussed by Steeds [2].

The recent introduction of the Philips EM400T has made the formation of small probes easier and more convenient. In effect the microscope can be

TABLE IV Pattern symmetries by order of bright-field symmetry

Bright-field	Whole pattern	Dark-field		± G		Diffraction group	Point group
		General	Special	General	Special		
1	1	1	None	1	None	1	
				2_R	None	2_R	
2	1					1_R	
2	2	1	None			2	
		2	None			21_R	
m	1					m_R	
m	m	1	m	1	m	m	
				2_R	–	$2_R mm_R$	
2mm	m					$m1_R$	
2mm	2					$2m_R m_R$	
2mm	2mm	1	m			2mm	
		2	2mm			$2mm1_R$	
3	3	1	None	1	None	3	
				2_R	None	6_R	
3m	3					$3m_R$	
3m	3m	1	m	1	m	3m	
				2_R	–	$6_R mm_R$	
4	2					4_R	$\bar{4}$
4	4	1	None			4	4
		2	None			41_R	4/m
4mm	4					$4m_R m_R$	
4mm	2mm					$4_R mm_R$	
4mm	4mm	1	m			4mm	4mm
		2	2mm			$4mm1_R$	
6	3					31_R	$\bar{6}$
6	6	1	None			6	6
		2	None			61_R	6/m
6mm	3m					$3m1_R$	$\bar{6}$m2
6mm	6					$6m_R m_R$	622
6mm	6mm	1	m			6mm	6mm
		2	2mm			$6mm1_R$	6/mmm

operated in a mode similar to the STEM mode but still retains the ability to form images without refocussing the objective.

6. Determining the point group

It is best, although not necessary, to work with low index zone axes if possible. These zones display the higher symmetry elements of the particular point group, which makes analysis easier and it is also easier to orient exactly on a zone axis if high symmetries are present. It is also an aid to analysis if all the high symmetry, low index zone axes plus any other prominent axes are collected together and displayed on a stereographic projection or zone axis pattern map (ZAP map). This is useful for subsequent "finger print" identification of the particular phase. A ZAP map for the common stainless steel carbide precipitate, $M_{23}C_6$ is shown in Fig. 4.

In the easiest cases it is only necessary to consider single, on axis CBPs from sometimes one, more usually two or three high symmetry, low index zone axes to determine the point group. For example, if such a pattern had 6 mm bright-field symmetry and 6 whole pattern symmetry, this would indicate that the diffraction group was

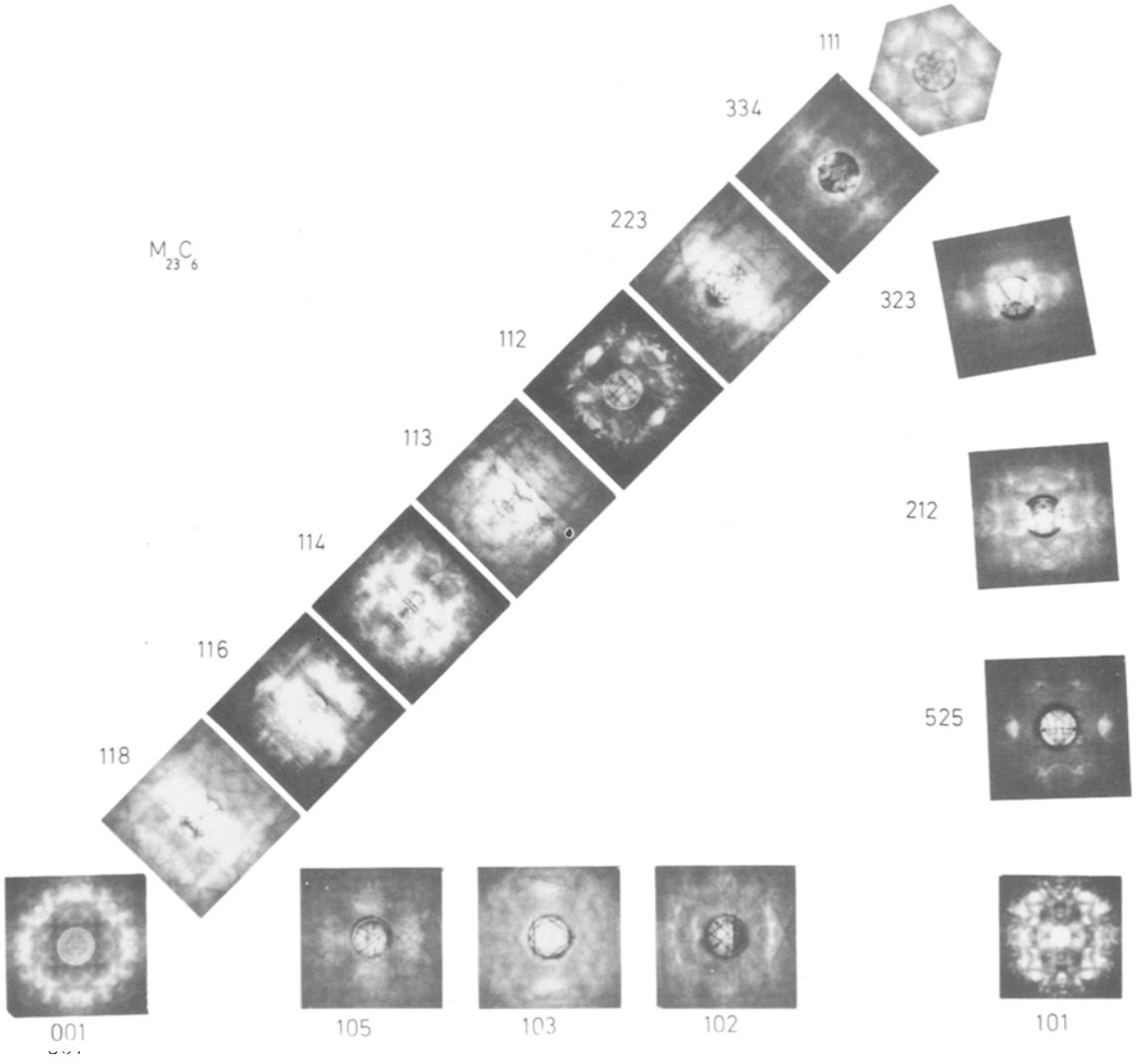

Figure 4 A convergent beam zone axis pattern map for $M_{23}C_6$.

$6m_Rm_R$ (Table I). From Table II, this can only come from the point group 6 2 2. For a practical example consider the ZAP map of $M_{23}C_6$. The [1 1 1] zone axis has 3m bright-field and 3m whole pattern symmetries. That is, the symmetry of the bright-field disc alone is 3m and the symmetry of the whole pattern, including bright-field and dark-field discs is 3m. Referring to Table I, it is seen that this can be produced by either 3m or 6_Rmm_R diffraction groups. From Table II, this leads to four possible point groups: 3m, $\bar{4}$3m, $\bar{3}$m and m3m. Now consider the [1 0 0] zone axis. This has 4mm bright field and 4mm whole pattern symmetries which Table I shows to be produced by either 4mm or $4mm1_R$ diffractions groups. From Table II the possible point groups are: 4mm, 4/mmm and m3m. Thus the point group of $M_{23}C_6$ is m3m, since only this group can produce both of the patterns observed. Note that in this case no information apart from the zone axis symmetries is necessary for determination of the point group.

If other information is known, such as the lattice type, which is often quite easy to determine, and the zone axes are indexed, this will help greatly. In this case Table III can be used. Consider FeCrB, the ZAP map of which is shown in Fig. 5. Indexing the CBPs reveals the crystal is orthorhombic, for which the possible point groups are; mmm, mm2, 222. The [1 0 0] zone axis has 2mm bright-field and whole pattern symmetries which can, according to Table I, come from either 2mm or $2mm1_R$ diffraction groups. From Table III it can immediately be seen that a [1 0 0] zone axis from any orthorhombic crystal can only

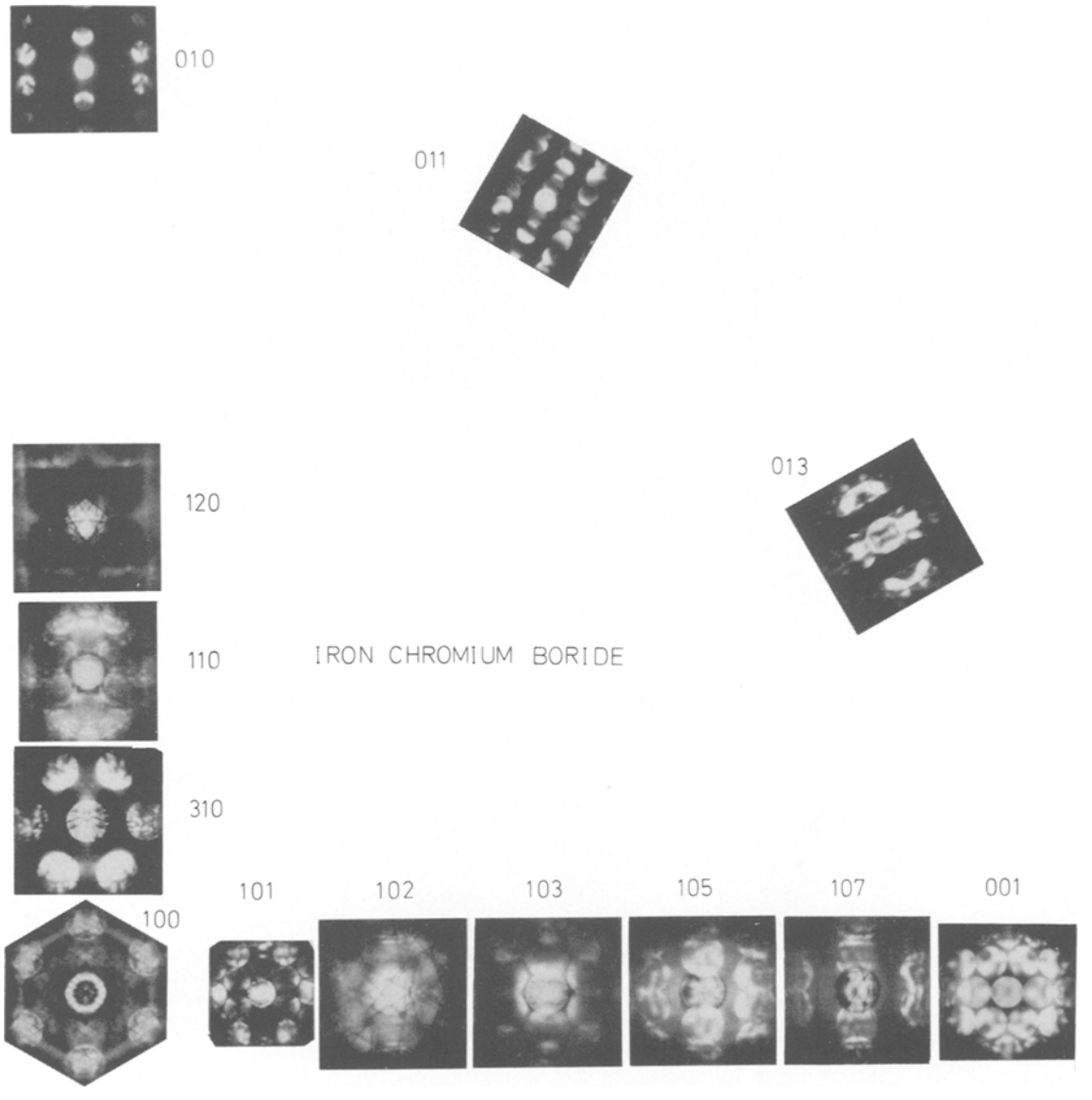

Figure 5 A convergent beam zone axis pattern map for FeCrB.

belong to diffraction groups $2mm1_R$, $m1_R$ or $2m_Rm_R$. Thus the correct diffraction group is $2mm1_R$ and the point group is mmm. This can be confirmed from the symmetries of the [U V O] zone axes. Note that the [0 0 1] zone axis is of limited use in this case since no hoLz lines are visible. Thus only the projected symmetry is displayed.

The methods of analysis used in these two examples will in fact work in the majority of cases. Although not previously noted, it is possible, given at least two low index zone axes containing hoLz detail, to distinguish 28 point groups on the basis of bright-field and whole pattern symmetries alone. The exceptions are the pair 1 and $\bar{1}$ and the pair 3 and $\bar{3}$. In these two cases, or when only one low index zone axis containing hoLz detail is available, as will often happen for the lower symmetry point groups, it is necessary to examine other symmetry elements of CBPs. In particular the symmetry of individual dark-fields becomes important. To determine the dark-field symmetry it is necessary to align the CBP so that the symmetry centre for the dark-field under consideration lies near the centre of the relevant dark-field disc. The symmetry centre is at the Bragg angle (Fig. 6) which is halfway between the dark-field and bright-field discs of the on-axis CBP. In

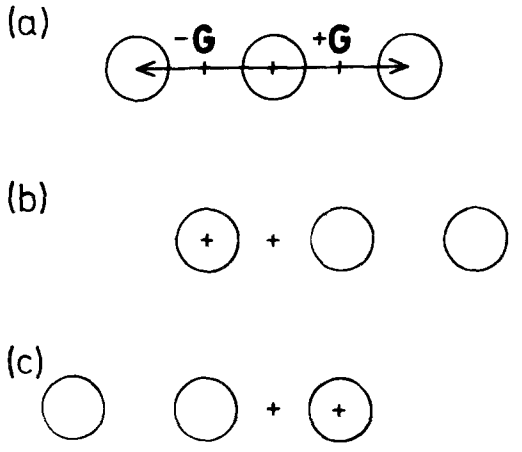

Figure 6 Diagramatic illustration of the determination of + G and − G dark-field symmetries.

principle it is possible to change the orientation of the specimen but this is very difficult to do accurately for the small angles involved. The easier method is to tilt the incident electron beam slightly by shifting the second condenser aperture and centring the dark-field on the Bragg angle. The dark-field symmetry will then be apparent. An example is shown in Fig. 7. Both the internal symmetry of the individual dark-field and the symmetry relation between + G and − G related dark-fields provide useful information. These dark-field symmetries are listed in Table I. Note that in certain special positions, which occur either along mirror lines in the CBP or along lines perpendicular to mirror lines, the symmetry of the dark-fields is increased. A full explanation of special positions is given by Buxton *et al.* [3].

It is useful to rearrange Table I in order of increasing bright-field and whole pattern symmetry. This is done in Table IV and in addition only necessary information is included. Note that for the higher symmetry CBPs there are a number of cases of one to one correspondence between diffraction group and point group. It is also important to note that the original analysis of Buxton *et al.* [3] is done in a fully dynamical fashion so that the results are valid in all diffraction situations, even if double diffraction effects are significant.

7. Determining space groups

Using CB methods it becomes easier to determine space groups than using conventional diffraction. The methods for observing screw axes and glide planes are outlined by Steeds *et al.* [4]. The

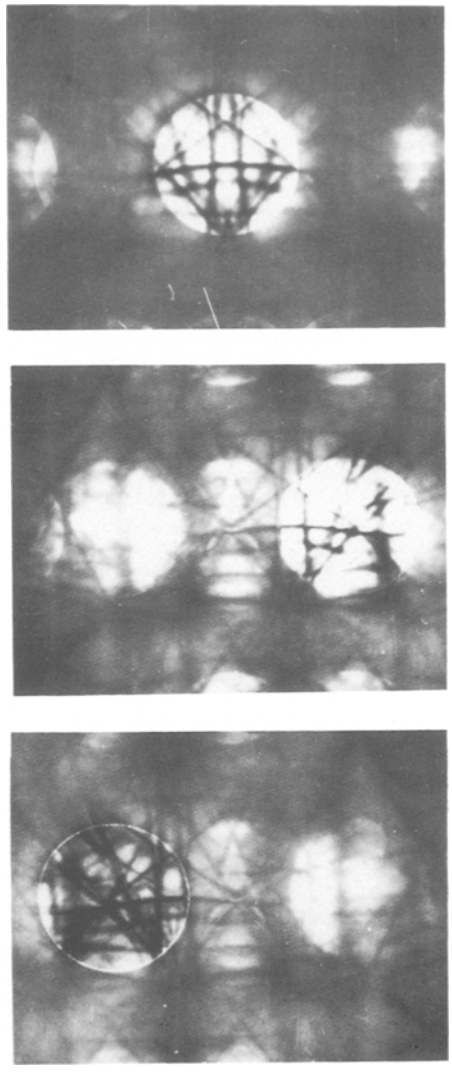

Figure 7 Example of the determination of + G and − G dark-field symmetries for the [5 2 5] zone axis of $M_{23}C_6$.

advantages of CB methods result from firstly the ease with which CBPs can be aligned exactly on the zone axis, a process which is very difficult to do with conventional diffraction methods, and secondly, and more important, the absence in the case of CBPs of any averaging over a range of angles. This occurs with conventional diffraction methods because the patterns come from a relatively large area, in contrast with CBPs, and unless the crystal is perfectly flat, a range of angles will be averaged in the resulting pattern. Thus in CBPs it is easier to locate absences due to the space group. Diffraction into space group forbidden discs can still occur but, whereas with conventional diffraction methods it is necessary to tilt

the specimen to determine if a diffraction spot is a result of double diffraction, for CBPs discs produced by double diffraction can often be distinguished without tilting the specimen. There are two types of double diffraction. In one type the double diffraction occurs by diffraction via zero layer interactions only. It is this mechanism which is usually responsible for intensity in the [0 0 0 1] reflections from hexagonal close packed structures, even though they are often space group forbidden. This mechanism results in the occurrence of crosses of zero intensity, occurring in the space group forbidden reflections when they are aligned at the Bragg angle. This indicates the presence of a screw axis or glide plane in the crystal. Steeds *et al.* [4] should be consulted for more details.

The second type of double diffraction is via the higher order Laue zones. This leads to the appearance of bright hoLz lines on a dark background at the position of the forbidden reflection, in contrast to the usual appearance of dark hoLz lines on a bright background for allowed reflections. This type of double diffraction is responsible for the weak reflection in the [0 0 1] zone axis of FeCrB.

8. Conclusions

Convergent beam diffraction is a very powerful and versatile technique for the study and analysis of crystal structure in the electron microscope. Although at first sight more difficult than conventional diffraction methods, it is not and is considerably more useful.

This paper provides an introduction to the application of convergent beam methods and lists sources of more detailed information which are necessary for more difficult studies.

Acknowledgements

I should like to thank Dr J. A. Eades and Dr J. W. Steeds for advice and helpful discussions on convergent beam electron diffraction methods. I would also like to thank the SRC for financial support during the period the research from which this paper originated was performed.

References

1. W. KOSSEL and G. MÖLLENSTEDT, *Ann. Phys.* **36** (1939) 113.
2. J. W. STEEDS, "Introduction to Analytical Electron Microscopy", edited by J. J. Hren, J. J. Goldstein and U. C. Joy, (Plenum Press, New York, 1979) Ch. 15.
3. B. F. BUXTON, J. A. EADES, J. W. STEEDS and G. M. RACKHAM, *Phil. Trans.* **281** (1976) 171.
4. J. W. STEEDS, G. M. RACKHAM and M. D. SHANNON, "Electron Diffraction 1927–1977" (Inst. Phys. Conf. Ser. No. 41, Institute of Physics, London, (1979) p. 135.
5. G. M. RACKHAM and J. A. EADES, *Optik* **47** (1977) 227.
6. M. D. SHANNON and J. W. STEEDS, *Phil. Mag.* **36** (1977) 279.
7. P. M. JONES, G. M. RACKHAM and J. W. STEEDS, *Proc. Roy. Soc. Lond.* **A354** (1977) 197.

Received 1 July and accepted 18 November 1980.